High Q/V_m hybrid photonic-plasmonic crystal nanowire cavity at telecommunication wavelengths

Chih-Kai Chiang[a], Yi-Cheng Chung[b], Pi-Ju Cheng[c,d], Chien-Wei Wu[a], Shu-Wei Chang[c] and Tzy-Rong Lin[a,b*]

[a]Institute of Optoelectronic Sciences, National Taiwan Ocean University, 20224, Keelung, Taiwan; [b]Department of Mechanical and Mechatronic Engineering, National Taiwan Ocean University, 20224, Keelung, Taiwan; [c]Research Center for Applied Sciences, Academia Sinica, 11529, Taipei, Taiwan; [d]Department of Photonics, National Chiao Tung University, 30010, Hsinchu, Taiwan.
[*]trlin@ntou.edu.tw

ABSTRACT

We have analyzed a hybrid photonic-plasmonic crystal nanocavity consisting of a silicon grating nanowire adjacent to a metal surface with a gain gap between. The hybrid plasmonic cavity modes are highly confined in the gap due to the coupling of photonic crystal cavity modes and surface plasmonic gap modes. Using the finite-element method, we numerically solve guided modes of the hybrid plasmonic waveguide at a wavelength of 1.55 μm. The modal characteristics such as waveguide confinement factors and modal losses of the fundamental hybrid plasmonic modes are explored as a function of the groove depth at various gap heights. After that, we show the band structure of the hybrid crystal modes, corresponding to a wide band gap of 17.8 THz. To effectively trap the optical modes, we introduce a single defect into the hybrid crystal. At a deep sub-wavelength defect length as small as 180 nm, the resonant mode exhibits a high quality factor of 566.5 and an ultrasmall mode volume of 0.00186 $(\lambda/n)^3$ at the resonance wavelength of 1.55 μm. In comparison to the conventional photonic crystal nanowire cavity in the absence of metal surface, the figure of merit Q/V_m is enormously enhanced around 15 times. The proposed nanocavities open up the opportunities for various applications with strong light-matter interaction such as nanolasers and biosensors.

Keywords: Surface plasmon, photonic crystal, resonant cavity, nanolaser, biosensor, nanowire

1. INTRODUCTION

Recently, lots of efforts have been made in the miniaturization of lasers to dimensions below the diffraction limit. Various nanolasers have attracted considerable interest due to their potential for compact integration intensity [1], extremely low power consumption [2], and ultra-fast modulation [3]. Plasmonic nanocavities that integrate surface plasmon polariton (SPP) with optical cavities usually significantly reduce the effective mode volume (V_m). With the advantage of SPP, various plasmonic cavities, especially utilizing the gap mode of SPP, have been investigated recently [4, 5]. However, the quality factor of this type of cavities is limited by parasitic loss of metal substrate. To achieve high Q/V_m, Oulton et al [6] lately demonstrated a deep subwavelength plasmonic nanolaser using a dielectric nanowire (NW) on top of a metal surface, which successfully bring about coherent light spot far below the diffraction limit.

In this work, we analyze a hybrid plasmonic nanocavity containing a silicon NW photonic crystal (PhC) near a metal surface. With the periodic dielectric lattice atop the metal layer, hybrid plasmonic crystals can be formed to support a complete two-dimensional band-gap [7] for the hybrid plasmonic structure. A defect is introduced into the PhC NW to further confine the optical energy. We firstly investigate the modal characteristics of the hybrid plasmonic guided modes at various gap heights and indentation depths using 3D finite-element method (FEM) [8]. We also solve for the band structure of the hybrid photonic-plasmonic crystal structure. As a small defect is introduced, a resonance mode forms and exhibits that strong confinement inside the active gap region with high quality factor near 566 and ultrasmall modal volume 0.0019 $(\lambda/n)^3$ are achievable. The high figure of merit Q/V_m of the proposed nanocavity (approximately 300000) boosts the light-matter interaction, which is of great importance in various applications such as cavity QED, nonlinear optics, low-threshold nanoscale lasers, optomechanical devices, biological sensors [9,10], and surface-enhanced Raman scattering (SERS) [11-13].

Physics and Simulation of Optoelectronic Devices XXIII, edited by Bernd Witzigmann, Marek Osiński, Fritz Henneberger, Yasuhiko Arakawa, Proc. of SPIE Vol. 9357, 93571J
© 2015 SPIE · CCC code: 0277-786X/15/$18 · doi: 10.1117/12.2078541

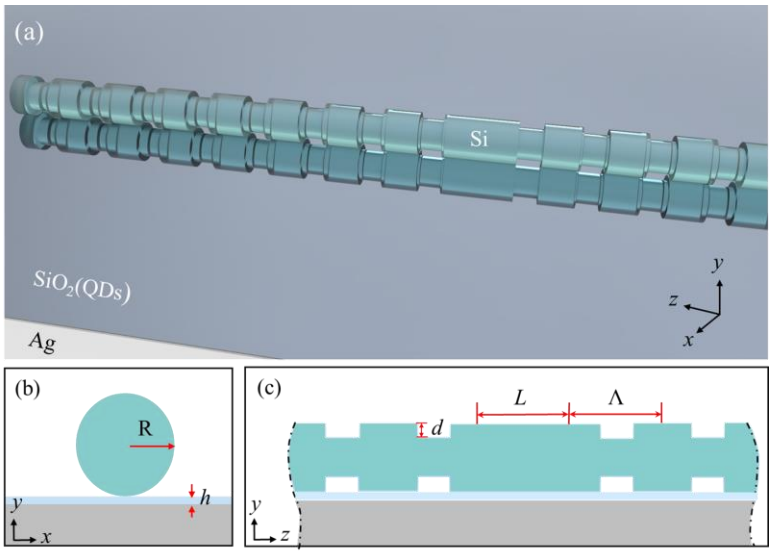

Figure 1. (a) The top (oblique) view, (b) front view (*x*-*y* plane), (c) side view (*y*-*z* plane) of the proposed nanocavity. A silicon NW with periodic dielectric lattice is placed on top of Ag substrate separated by the gap layer.

2. CHARACTERISTICS OF GUIDED MODES

The proposed hybrid plasmonic nanocavity is illustrated in Fig. 1. The structure consists of a patterned silicon NW and a silicon dioxide gap layer on flat silver substrate. The patterned NWs function as one-dimensional PhCs. The Si NW-SiO_2-silver film structure supports hybrid modes whose electric field intensity is strongly confined within the gap layer made of low-index gain medium. The hybrid plasmonic gap modes are coupled to the dielectric NW PhC Bloch modes to form a hybrid plasmonic crystal. As shown in Fig. 1, several dimensions of the proposed structure such as the NW etch depth d, the gap layer thickness h, and lattice constant Λ are varied to realize the optimal design of high Q-factor and low mode volume. Besides, the radius R of the Si NW is fixed at 150 nm.

To achieve high-reflection Bragg diffraction, we look for the high refractive index contrast along the NWs. Therefore, the indentation depth d is varied for finding the suitable corresponding effective index n_{eff}. As shown in Fig. 2, we solved for the n_{eff}, propagation lengths, WG confinement factors and mode areas with regard to various d and gap height h. As d is minimal, the parameters correspond to a bare NW of R =150 nm put upon the gap and metallic substrate. The hybrid plasmonic structure as high-low-index dielectrics on a metal substrate brings about even small footprint concentrated inside the low-index region. The plasmonic gap mode has the highest effective refractive index (Re[n_{eff}] = 2.2) and magnificent waveguide confinement factor. When we increase the etch depth, the air gap is enlarged and more electric field distributes over the low-index air region underneath the NW. The confinement inside the gain region therefore drops. The coupling strength of fundamental hybrid plasmonic gap mode is otherwise affected by the gap layer thickness h. For a smaller h, the better confinement underneath the NW leads to higher confinement factor and mode area. As shown in Figs. 2 (a) and (b), at an etch depth d higher than 40 nm, the NW guided mode has cut-off and the fields of hybrid mode leak into the ambience. The propagation distance hence falls quickly. On the other hand, at a moderate d, the propagation distance can be as long as one hundred micrometer. For the better confinement and lower modal loss of the fundamental hybrid plasmonic mode, we choose d as 40 nm and a moderate gap height h as 10 nm. The corresponding effective index Re[n_{eff}] is 1.15, which is much smaller than the index of the unetched NW (d = 0). This high index contrast ensures the formation of a large TM band gap when we introduce PhC structure into the NW hybrid plasmonic WG.

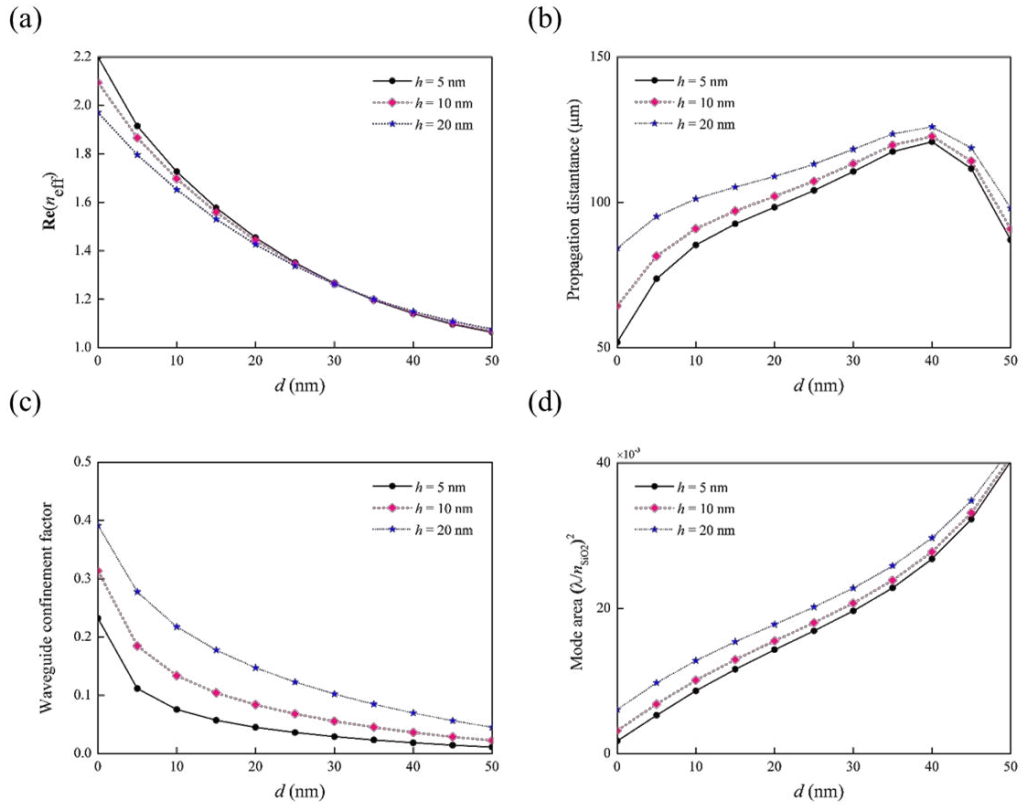

Figure 2. (a) The real part of effective index (b) propagation distance (c) WG confinement factor (d) mode area of the fundamental plasmonic hybrid gap mode as a function of the groove depth d for wire radius R = 150 nm and gap heights h = 5, 10 and 20 nm.

3. CAVITY DESIGN

Fig. 1(c) shows the unit cell of dielectric NW PhCs by engraving periodically on the circular surface along the z-axis [14]. The lattice constant Λ of a unit cell is 450 nm and the width of each indentation is 270 nm that are determined from Bragg condition. The filling factor is chosen so as to maximize the TM band gap and shift the band gap center to the target wavelength. In Fig. 3, we show the band structure of the hybrid crystal for both TM and TE polarizations. A band gap is clearly visible from 179.8 to 207.6 THz between the fundamental TM modes and first-order TM modes while some higher order modes below the light cone (the region above light blue line) are also illustrated. Figure 4 plots the corresponding field distributions ($|\mathbf{E}|$) of 4 lowest band-edge modes at the Brillouin zone boundary. The lowest two modes correspond to TM-polarized hybrid plasmonic Bloch modes with the major electric field element E_y, and the higher two modes are TE-polarized with the major electric field element E_x. In contrast to the TE modes illustrated in Figs. 4 (c) (d), the TM band-edge modes in Figs. 4(a) (b) strongly concentrated inside the low-index gap region underneath the NW.

Based on the band structure of the hybrid plasmonic crystals shown in Fig. 3, we designed a defect cavity to support the resonant modes which are strongly squeezed into the gap region. In order to increase the concentration of optical energy in the nanocavity, different number of periods of each side by the cavity is varied to resolve the corresponding reflectivity by using 3D FEM and orthogonality theorem [4]. The result shows that the reflectivity is proportional to the number of periods and gradually convergent. We obtain sufficiently small mirror loss when the cavity is accompanied with a pair of gratings of 8 periods. For the hybrid plasmonic nanocavity, we examine the Q factor of the resonant mode at a defect length L = 270 nm by carrying out 3D FEM calculations. We then look into the field profiles of the high-Q resonant mode at λ = 1550 nm, which is potentially more promising for lasing. As shown in Fig. 5, the side view (y-z plane) of the field profiles of the cavity eigenmode reveals strong localization below the NW, whereas the top-view (x-z plane) shows that the field quickly decays inside the mirror region. Only one eigenmode with even symmetry along the

z-axis is supported in this cavity. In addition, we solved for the quality factor Q of the nanocavity. In 3D FEM calculations, we excited the nanocavity with a $\hat{y}$-polarized plane wave. The spatial integration of the squared magnitude of the electric field (proportional to electric energy density) inside the gain region was then recorded in the Fig. 6 when the wavelength was changed through the resonance. The Q factor was calculated from the ratio between the full width at half maximum (FWHM) and the peak resonance wavelengths of the corresponding lineshape. Finally, resolving the field distributions of the resonance modes enables us to obtain the mode volume V_m [15].

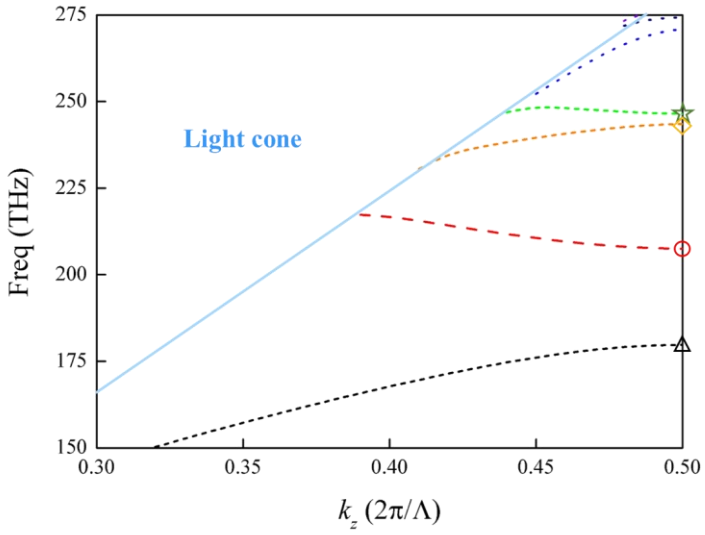

Figure 3. The band structure of the hybrid plasmonic crystals for the lattice constant. The lower two bands correspond to TM bands, and the higher two bands are TE bands. The light cone is indicated by the region above the blue line.

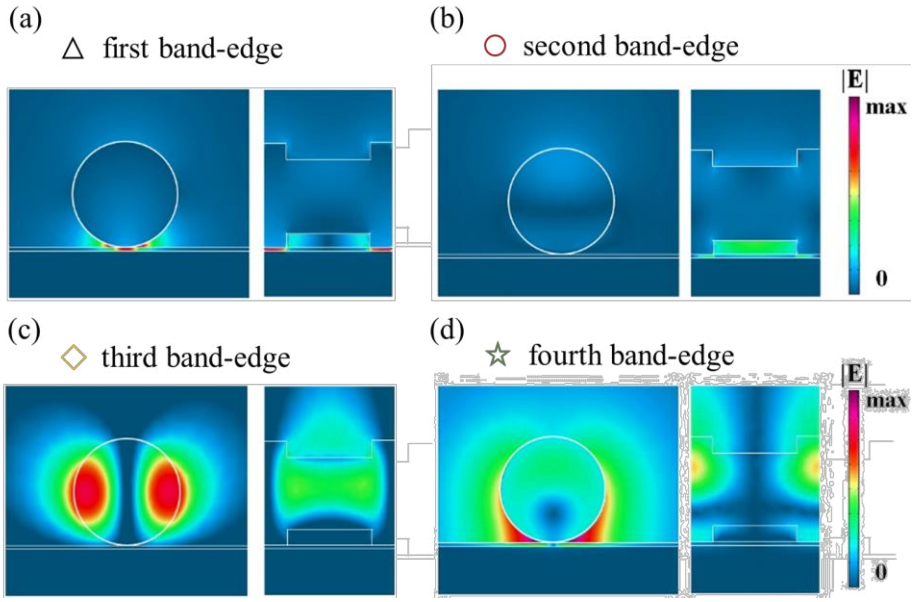

Figure 4. The corresponding field distributions (|**E**|) of the (a) first, (b) second, (c) third and (d) fourth band-edge mode at the Brillouin zone boundary as shown in Fig. 3.

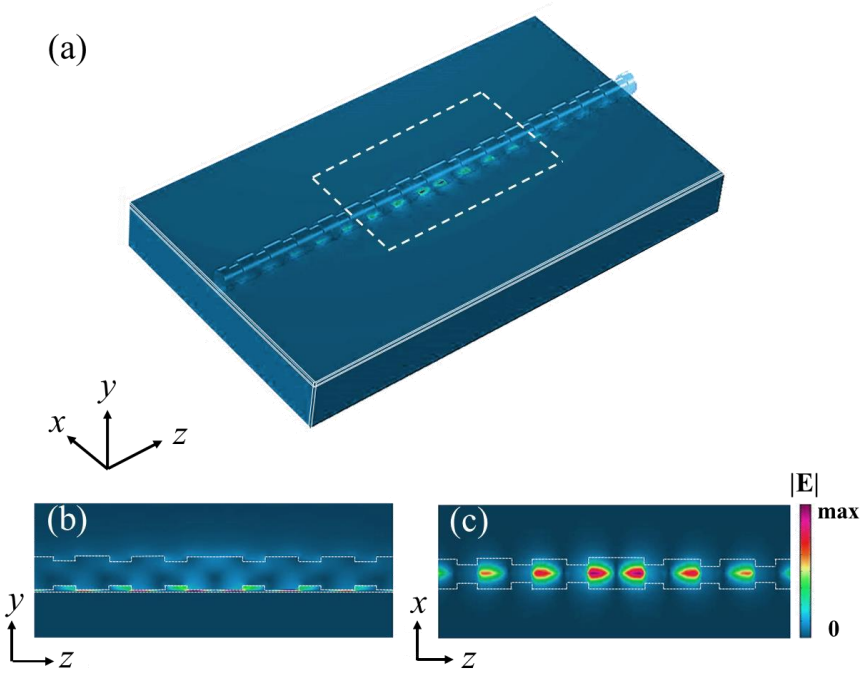

Figure 5. (a) The oblique top view, (b) side view (*y*-*z* plane), and (c) top view (*x*-*z* plane) of the mode profiles corresponding to the case of cavity length L = 270 nm at the middle of the gap layer.

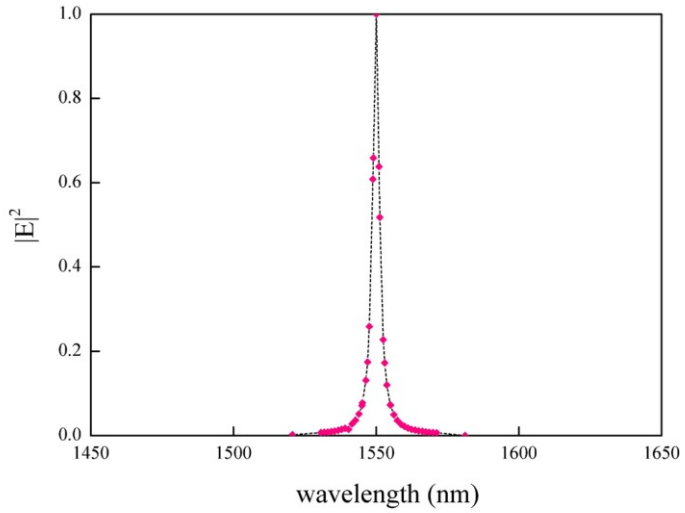

Figure 6. The resonance line shape calculated from 3D FEM for the mode at cavity length L = 270 nm and h = 10 nm. The corresponding quality factor is approximately 566.5.

4. CONCLUSIONS

We analyze a hybrid photonic-plasmonic crystal nanocavity containing a silicon grating nanowire near a metal surface with a gain gap between. We analyze the modal characteristics of the hybrid plasmonic waveguide modes at various gap heights and groove depths using finite-element method. We also numerically solve the bandstructure of the hybrid crystal modes. As a single defect is introduced to the photonic crystal, a cavity mode forms and exhibits strong confinement inside the active gap region. For such cavities with a short defect length, a high quality factor near 567 and ultrasmall modal volume lower than 0.0019 $(\lambda/n)^3$ are achievable.

ACKNOWLEDGMENT

This work was sponsored by National Taiwan Ocean University, Research Center for Applied Sciences, Academia Sinica, Taiwan, and Ministry of Science and Technology, Taiwan under Grant number MOST 103-2221-E-019-028-MY3.

REFERENCES

[1] Nezhad, M. P., Simic, A., Bondarenko, O., Slutsky, B., Mizrahi, A., Feng, L., Lomakin, V. and Fainman, Y., "Room-temperature subwavelength metallo-dielectric lasers," Nature Photon. **4**, 395-399 (2010).
[2] Park, H. G., Kim, S. H., Kwon, S. H., Ju, Y. G., Yang, J. K., Baek, J. H., Kim, S. B. and Lee, Y. H., "Electrically driven single-cell photonic crystal laser," Science **305**, 1444-1447 (2004).
[3] Englund, D., Altug, H., Ellis, B. and Vuckovic, J., "Ultrafast photonic crystal lasers," Laser & Photon. Rev. **2**, 264-274 (2008).
[4] Jiang, H. Q., Liu, C., Wang, P., Zhang, D. G., Lu, Y. H. and Ming, H., "High-Q/V_{eff} gap-mode plasmonic FP nanocavity," Opt. Express **21**, 4752-4757 (2013).
[5] Cheng, P. J., Weng, C. Y., Chang, S. W., Lin, T. R. and Tien, C. H., "Plasmonic gap-mode nanocavities with metallic mirrors in high-index cladding," Opt. Express **21**, 13479-13491 (2013).
[6] Oulton, R. F., Sorger, V. J., Zentgraf, T., Ma, R. M., Gladden, C., Dai, L., Bartal, G. and Zhang, X., "Plasmon lasers at deep subwavelength scale," Nature **461**, 629-632 (2009)
[7] Yang, X., Ishikawa, A., Yin, X. and Zhang, X., "Hybrid photonic-plasmonic crystal nanocavities," ACS Nano **5**, 2831-2838 (2011)
[8] COMSOL Multiphysics [http://www.comsol.com/]
[9] Sun, C., Su, K.-H., Valentine, J., Rosa-Bauza, Y. T., Ellman, J. A., Elboudwarej, O., Mukherjee, B., Craik, C. S., Shuman, M. A., Chen, F. F. and Zhang, X., "Time-resolved single-step protease activity quantification using nanoplasmonic resonator sensors," ACS Nano **4**, 978-984 (2010).
[10] McPhillips, J., Murphy, A., Jonsson, M. P., Hendren, W. R., Atkinson, R., Hook, F., Zayats, A. V. and Pollard, R. J., "High-performance biosensing using arrays of plasmonic nanotubes," ACS Nano **4**, 2210-2216 (2010)
[11] Maier, S. A., "Plasmonic field enhancement and SERS in the effective mode volume picture," Opt. Express **14**, 1957-1964 (2006)
[12] Lee, S. Y., Hung, L., Lang, G. S., Cornett, J. E., Mayergoyz, I. D. and Rabin, O., "Dispersion in the SERS enhancement with silver nanocube dimers," ACS Nano **4**, 5763-5772 (2010)
[13] Gehan, H., Fillaud, L., Chehimi, M. M., Aubard, J., Hohenau, A., Felidj, N. and Mangeney, C., "Thermo-induced electromagnetic coupling in gold/polymer hybrid plasmonic structures probed by surface-enhanced Raman scattering," ACS Nano **4**, 6491-6500 (2010)
[14] Christesen, J. D., Pinion, C. W., Grumstrup, E. M., Papanikolas, J. M. and Cahoon, J. F., "Synthetically encoding 10 nm morphology in silicon NWs," Nano Lett. **13**, 6281-6286 (2013).
[15] Robinson, J. T., Manolatou, C., Chen, L. and Lipson, M., "Ultrasmall mode volumes in dielectric optical microcavities," Phys Rev Lett **95**,143901 (2005).